

## PHOTOIONIZATION DETECTOR FOR GAS CHROMATOGRAPHY

## I. DETECTION OF INORGANIC GASES

MIKIYA YAMANE

*Hitachi Central Research Laboratory Kokubunji,  
Tokyo (Japan)*

(Received October 8th, 1963)

Two previous papers<sup>1,2</sup> described properties of the argon ionization detector, in which the radioactive source is replaced by a gaseous discharge in the vicinity of the sensing electrodes. It was shown that the detector was based on the same reactions as those of LOVELOCK's argon ionization detector<sup>3</sup>, except that primary electrons were supplied from the discharge.

There has been, however, added interest in this type of device since the discharge excited in inert gases emits ultraviolet radiation with energies above the ionization potentials of solute molecules. This implies that the radiation can produce ionization when passing through the solute gases. This fact has been made the basis of a new detector by LOVELOCK<sup>4</sup>, but little information on the performance characteristics of the detector has been published.

The present work has been directed toward finding a practical photoionization detector by modifying its predecessors<sup>2</sup>. The modification was made in such a way that only light emitted from the discharge can pass through the sensing region while charged particles generated by the discharge are inhibited from flowing to the sensing electrodes.

The detector as modified was operated using helium as both the discharge and the carrier gas, and it was found that the photoionization method can be applied with considerable advantages over other techniques to the detection of wide variety of substances and that it is particularly well suited to the investigation of inorganic gases, the detection of which is difficult by other techniques when only small quantities are present.

## APPARATUS

Figs. 1(A) and 1(B) show the photoionization detector used, a modified version of those previously described<sup>2</sup>. The detector consists of two glass chambers, one of which is the discharge chamber and the other the sensing chamber, and is provided with the inlets for the discharge and the carrier gas and a common outlet. In the discharge chamber is mounted a pair of 0.5 mm Kovar wires, the ends of which are bent toward each other (gap distance approximately 0.1 mm), so that the discharge may be fixed there. The anode in the sensing chamber is made of a Kovar pipe of 1.5 mm o.d. and 1 mm i.d. The cathode is a semi-spherical nickel dish with a radius of 2.5 mm.

The two chambers are joined together by a funnel-shaped Kovar pipe, so that the

light beam from the discharge may traverse through the space between the sensing electrodes. The light, however, does not irradiate the surface of the sensing electrode and thus photoelectric emission from the sensing electrodes is negligible. This pipe is electrically grounded and acts as an electrode that prevents charged particles from flowing into the sensing chamber (hereafter this pipe is called the ion trap).

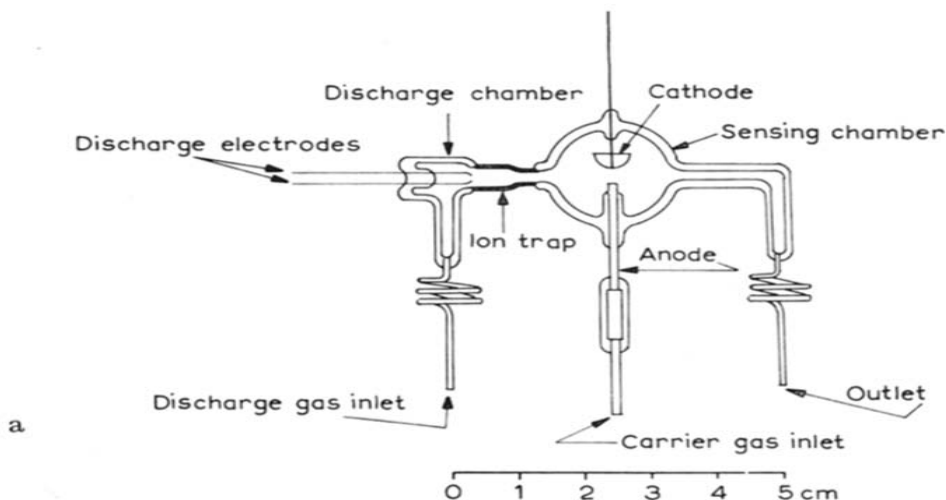


Fig. 1 (A). Construction of photoionization detector.

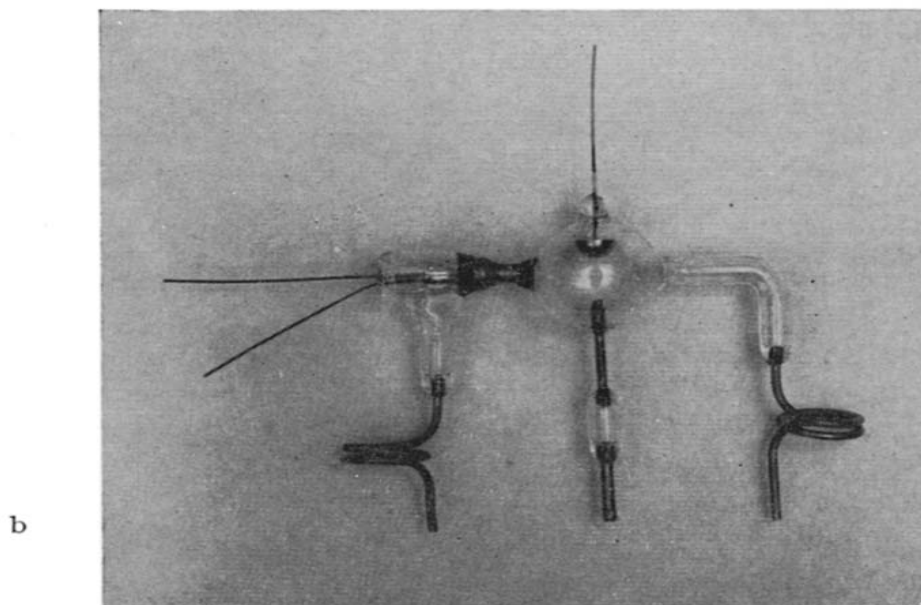


Fig. 1 (B). Photoionization detector.

The basic arrangement of the apparatus used for measuring the photoionization current of solute molecules is the same as that described in the previous paper<sup>2</sup>. The apparatus incorporates two separate gas flows, namely, the discharge gas flow and the carrier gas flow. In all the measurements helium was used as both the discharge and the carrier gas for two reasons.

(1) As discovered by HOPFIELD<sup>5</sup> and studied by TANAKA *et al.*<sup>6-8</sup>, the discharge in helium at high pressures emits a continuum of radiation in the wavelength region

between *ca.* 600 and 1100 Å, photons of the highest energies that can be obtained under the simple discharge condition. This continuum can profitably be used to ionize all kinds of molecules except those of helium and neon.

(2) These photons should not be absorbed by the carrier gas, as this would reduce the ionization efficiency of the solute gases. The use of helium as the carrier gas satisfies this requirement and, moreover, should not give any background current in the absence of solute gases.

Precautions were taken to remove impurities from helium by incorporating an impurity trap into each of the gas flows. These traps were copper columns (1 m × 4 mm i.d.) packed with activated charcoal. After activation (by heating to 200° for about 1 h), they were immersed in liquid nitrogen.

#### EXPERIMENTAL RESULTS

##### *Background current*

In principle, the background current of the photoionization detector should be zero in the absence of solute gases, since charged particles generated by the discharge are inhibited from flowing into the sensing chamber. In order to check this prediction, measurements were made of the background current-anode voltage characteristic under the following conditions:

Carrier gas	= He 30 ml/min.
Discharge gas	= He 0, 50, 100, 150 ml/min.
Discharge current	= 30 $\mu$ A.
Ion trap voltage	= 0 V.
Impurity trap	= Activated charcoal 1 m (—196°).
Column	= Molecular sieve 13X 1.5 m (20°).

The results plotted in Fig. 2 show that the background current in the saturation region is of the order of  $10^{-10}$  to  $10^{-9}$  A.

It can be seen that all the curves pass through the origin, indicating that the effect of the electrical force between the discharge and the sensing chamber<sup>2</sup> is entirely eliminated by the earthed ion trap.

It is clear from Fig. 2 that the background current varies with the discharge gas flow, and that in the four curves a maximum current is obtained at a flow rate of 50 ml/min. To investigate the matter further, gas-flow dependence studies were made under the same conditions, while the anode voltage was kept constant and the gas flow rate was varied. The results of measurements at three different anode voltages are shown in Fig. 3. The curves in Fig. 3 show that with increasing gas flow the background current increases at first, reaches a maximum at *ca.* 50 ml/min and then decreases. This trend of the curves is not in accordance with the previous investigations where the background current increased continually with the gas flow. It can be interpreted in terms of photoionization of impurities which, in spite of purification by the cold impurity traps, are entrained by both the carrier and the discharge gas.

There are two possible causes for the initial rise of the background current. (1) The discharge gas is contaminated with impurities that come from the wall of the tube or from the impurity trap. These impurities when present between the discharge and the sensing chamber can absorb photons, thus reducing the intensity of ultra-

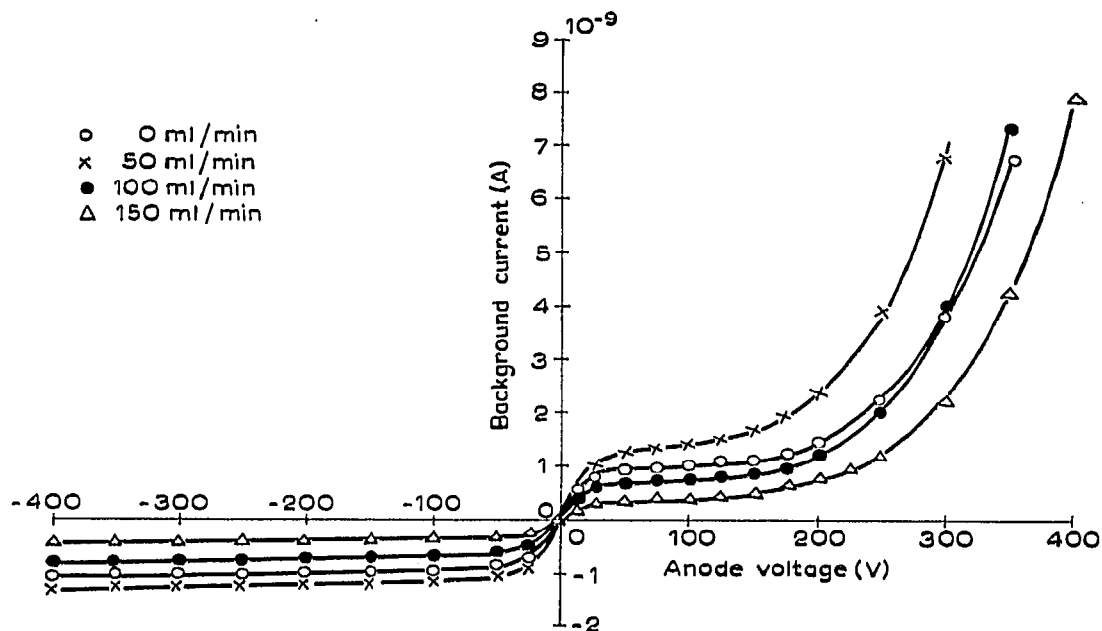


Fig. 2. Background current as a function of the anode voltage. Carrier gas = He 30 ml/min; discharge gas = He 0, 50, 100, 150 ml/min; discharge current =  $30 \mu\text{A}$ ; impurity trap = activated charcoal ( $-196^\circ$ ); column = molecular sieve 13X 1.5 m ( $20^\circ$ ).

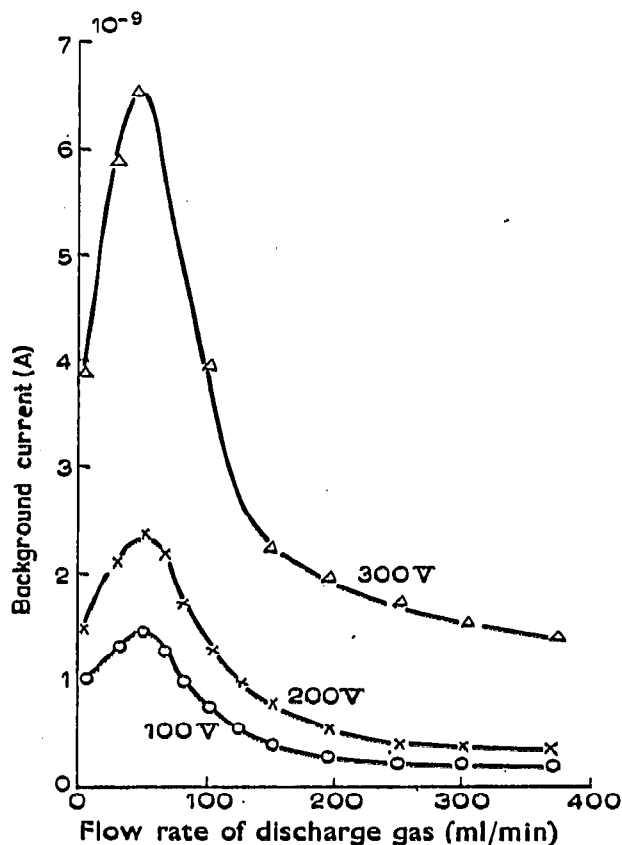


Fig. 3. Background current as a function of the flow rate of the discharge gas. Carrier gas = He 30 ml/min; discharge current =  $30 \mu\text{A}$ ; anode voltage = 100, 200, 300 V; impurity trap = activated charcoal ( $-196^\circ$ ); column = molecular sieve 13X 1.5 m ( $20^\circ$ ).

violet radiation that passes through the sensing region. The increase in the discharge gas flow dilutes the impurity and increases the radiation intensity. (2) The carrier gas is much more contaminated with impurities than the discharge gas, as it has passed through a sample port and a chromatographic column. At lower discharge gas flows, the carrier gas that has flowed in the sensing chamber can diffuse towards the discharge chamber counter to the discharge gas flow. The effect of this counter-flow diffusion is to reduce the intensity of ultraviolet radiation because of absorption by the impurities contained in the diffusing carrier gas. The increase in the discharge gas flow suppressed the counter-flow diffusion of the carrier gas and increases the radiation intensity.

The increase in the background current with the discharge gas flow continues until the dilution of the impurities in the sensing chamber becomes appreciable. Thereafter, further reduction of the concentration causes a lowering of ionization. The decrease in the background current with higher discharge gas flows is attributable to this effect.

#### *Effect of the impurity traps*

As would be expected from the results of the foregoing measurements of the background current, the output signal of the detector should be influenced by the impurities contained in both the discharge and the carrier gas. To study this effect, chromatograms were taken, setting the temperature of the impurity traps to different values and operating the detector under constant conditions.

Fig. 4 shows two typical chromatograms of 0.1 ml of coal gas. The impurity traps of the two gas flows were kept at room temperature (right chromatogram) and then

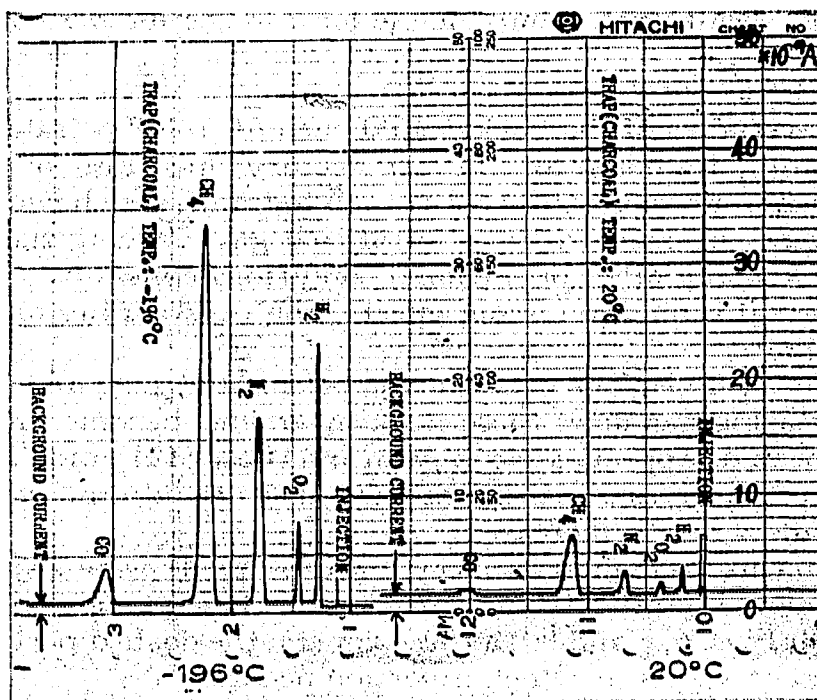


Fig. 4. Chromatograms of 0.1 ml of coal gas showing the effect of the impurity traps. Full scale =  $50 \cdot 10^{-9}$  A. Carrier gas = He 30 ml/min; discharge gas = He 150 ml/min; discharge current = 60  $\mu$ A; anode voltage = 100 V; column = molecular sieve 13X 1.5 m (20°).

cooled to liquid nitrogen temperature (left chromatogram). Other operational conditions were as follows:

Carrier gas	= He 30 ml/min.
Discharge gas	= He 150 ml/min.
Discharge current	= 60 $\mu$ A.
Anode voltage	= 100 V.
Ion trap voltage	= 0 V.
Column	= Molecular sieve 13X 1.5 m (20°).

In both of these chromatograms, signal currents corresponding to hydrogen, oxygen, nitrogen, methane and carbon monoxide appear as a positive deflection. These ionization peaks can only come from the photoionization process, since it is not believed that ionization by collision of electrons could take place at an anode voltage of 100 V.

The effect of the gas treatment on the output signal is quite clearly shown in Fig. 4: corresponding ionization peaks in the two chromatograms differ by a factor of about 10. This difference can be attributed to the fact that, with the impurity traps kept at room temperature, permanent gases cannot be removed from the discharge gas. Such impurities absorb ultraviolet light and decrease the number of photons passing through the sensing chamber, so that ionization peaks must be diminished.

It is to be noted that the background current in the right chromatogram is about two times as great as that in the left chromatogram. This observation is consistent with the view that the background current is determined by the concentration of the impurities.

Owing to these observations, all measurements described below were conducted with the impurity traps immersed in liquid nitrogen, and it was found that, with proper precautions, results were reproducible for a long time period of operation.

#### *Effect of the discharge gas flow*

As indicated in the studies of the background current, the flow rate of the discharge gas is an important parameter for the satisfactory operation of the detector. To illustrate this effect, four representative chromatograms are shown in Fig. 5. These chromatograms were obtained with 0.1 ml of coal gas, varying the flow rate of the discharge gas and keeping other operational conditions constant.

These data reveal some interesting effects; the outstanding ones can be briefly summarized as follows.

- (1) At 30 ml/min, inversions occur in the peaks of H<sub>2</sub>, N<sub>2</sub> and CH<sub>4</sub>.
- (2) With increasing gas flow, these peak inversions become diminished; the inversion of the N<sub>2</sub> peak disappears at 70 ml/min and those of H<sub>2</sub> and CH<sub>4</sub> at 150 ml/min.
- (3) The peak of O<sub>2</sub> gives a maximum current at 70 ml/min, while that of CO is diminished as the flow rate is increased.

In addition to this preliminary survey, measurements were also made for H<sub>2</sub>, O<sub>2</sub> and N<sub>2</sub> to obtain more quantitative information on these phenomena. The results obtained are shown in Figs. 6, 7 and 8. In these figures, the dashed portions of the curves correspond to current values at which inversion occurs.

It can be seen from these figures that, with increasing gas flow, the peak current increases at first, reaches a maximum and then decreases. This is similar to the background current *vs.* gas flow characteristic.

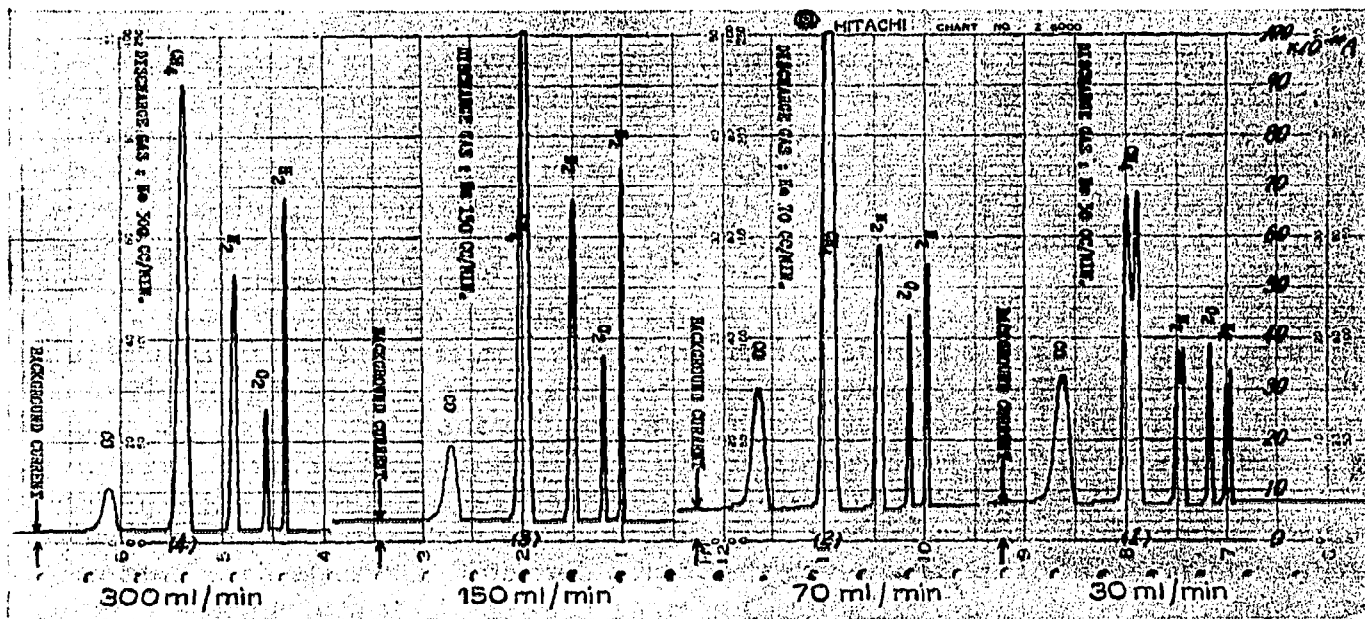


Fig. 5. Chromatograms of 0.1 ml of coal gas showing the effect of the discharge gas flow. Full scale =  $100 \cdot 10^{-10}$  A. Carrier gas = He 30 ml/min; discharge current =  $30 \mu\text{A}$ ; anode voltage = 100 V; column = molecular sieve 13X 1.5 m ( $20^\circ$ ).

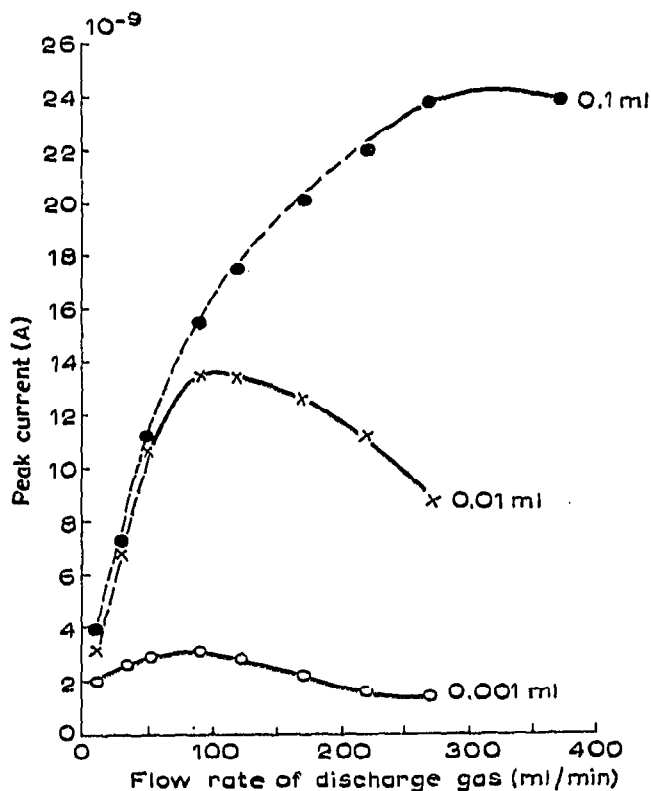


Fig. 6. Effect of the flow rate of the discharge gas on the peak current of  $\text{H}_2$ . Sample quantity = 0.1, 0.01, 0.001 ml; carrier gas = He 30 ml/min; discharge current =  $30 \mu\text{A}$ ; anode voltage = 100 V; column = molecular sieve 13X 1.5 m ( $20^\circ$ ).

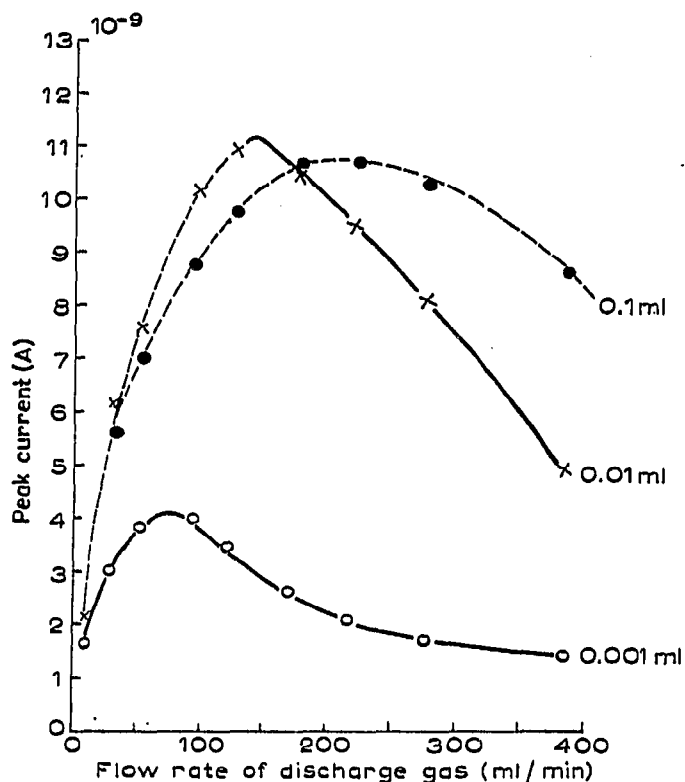


Fig. 7. Effect of the flow rate of the discharge gas on the peak current of O<sub>2</sub>. Sample quantity = 0.1, 0.01, 0.001 ml; carrier gas = He 30 ml/min; discharge current = 30  $\mu$ A; anode voltage = 100 V; column = molecular sieve 13X 1.5 m (20°).

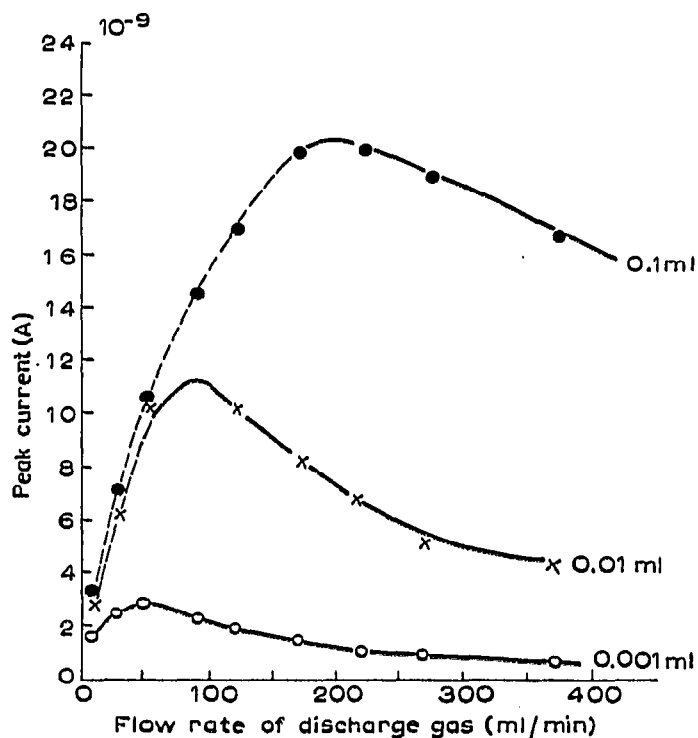


Fig. 8. Effect of the flow rate of the discharge gas on the peak current of N<sub>2</sub>. Sample quantity = 0.1, 0.01, 0.001 ml; carrier gas = He 30 ml/min; discharge current = 30  $\mu$ A; anode voltage = 100 V; column = molecular sieve 13X 1.5 m (20°).



With this similarity as a basis, we can interpret the experimental curves as follows. The discharge gas has two effects, that of increasing the number of photons that pass through the space between the sensing electrodes and that of reducing the concentration of the sample gas in the sensing chamber. The initial increase in the current at lower discharge gas flows is caused by the former effect. The latter effect is, of course, to reduce the ionization efficiency; this accounts for the slow decline in the region of higher discharge gas flows. These opposing effects should yield a maximum point on the current-gas flow curves.

The peak inversion that is likely to occur when the gas flow is low, and when the sample quantity is large, is attributed to the diffusion of the sample gas counter to the discharge gas flow. As the density of the sample gas in the sensing chamber is increased, the rate of the counter-flow diffusion increases, and fractions of the diffusing sample gas can move closer to the discharge chamber. Thus, with increasing density of the sample gas, the absorption of ionizing photons increases to a stage where the resulting ions cannot be collected by the ion collector, but are captured by the ion trap or recombine with electrons. This reduces the effective radiation intensity in the sensing region, resulting in a decrease in ion current at higher densities of the sample gas.

#### *Effect of the anode voltage*

Fig. 9 shows the peak current as a function of the anode voltage for 0.01 ml of  $H_2$ ,  $O_2$  and  $N_2$ . It can be seen that  $H_2$  and  $N_2$  yield a saturation current below *ca.* 300 V, while for  $O_2$  the current increases, though slightly, as the anode voltage is increased.

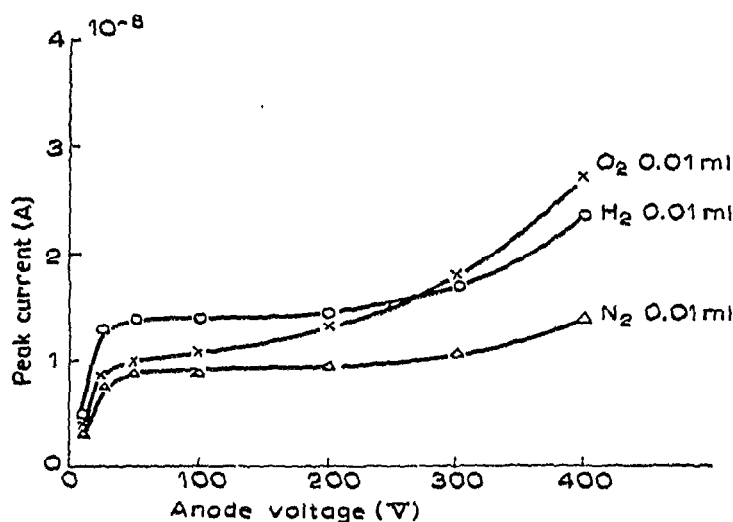


Fig. 9. Effect of the anode voltage on the peak current of  $H_2$ ,  $O_2$  and  $N_2$ . Sample quantity = 0.01 ml; carrier gas = He 30 ml/min; discharge gas = He 150 ml/min; discharge current = 30  $\mu$ A; column = molecular sieve 13X 1.5 m (20°).

The signal to background ratio that can be obtained from Figs. 2 and 9 decreases with increasing anode voltage; the value for 0.01 ml of  $H_2$ , for instance, varies from *ca.* 45 at 100 V to *ca.* 3 at 400 V. Since increase in the background current is expected to increase the noise level, it is advisable to operate the detector at lower anode voltages.

*Sensitivity and limit of detection*

The relation between the output current and the sample quantity was determined for  $H_2$ ,  $O_2$  and  $N_2$ . These sensitivity studies were made with  $H_2$ -air mixtures of different compositions, which were introduced by means of a sample port of 0.1 ml.

Fig. 10 shows a series of chromatograms that covers the range of  $H_2$  concentration from 1 to 0.1% (1-0.1  $\mu$ l). Fig. 11 also shows two chromatograms of air- $H_2$

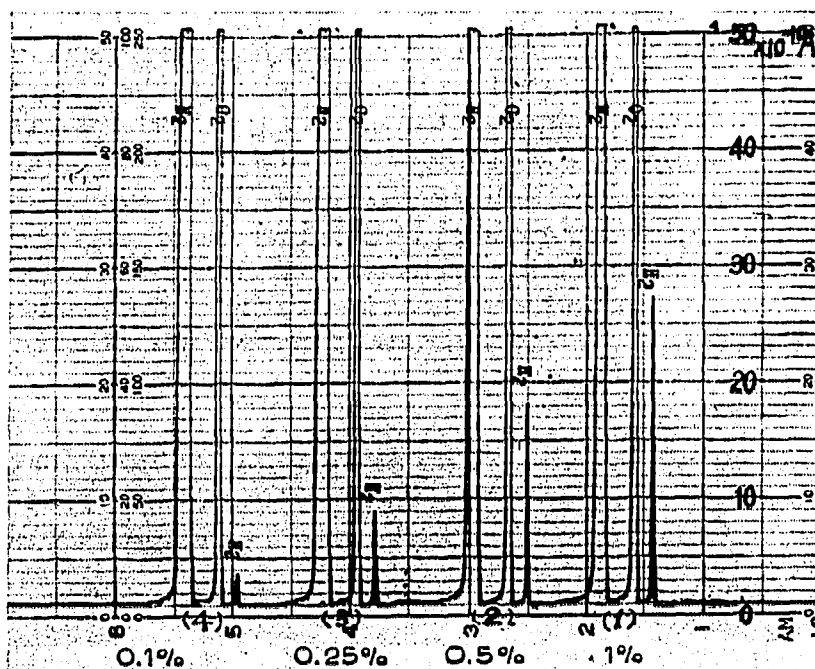


Fig. 10. Chromatograms of 0.1 ml of  $H_2$ -air mixtures. Full scale =  $50 \cdot 10^{-10}$  A. (1)  $H_2$  1%; (2)  $H_2$  0.5%; (3)  $H_2$  0.25%; (4)  $H_2$  0.1%. Carrier gas = He 30 ml/min; discharge gas = He 150 ml/min; discharge current =  $30 \mu$ A; anode voltage = 100 V; column = molecular sieve 13X 1.5 m ( $20^\circ$ ).

(100:0.1) and air- $H_2$  (100:0.05) analogous to those in Fig. 10, except that the ordinate scale is expanded by a factor of 10. It can be seen that 0.1  $\mu$ l of  $H_2$  gives a peak current of  $3.5 \cdot 10^{-10}$  A while the noise level was found to be about  $3 \cdot 10^{-13}$  A. This indicates that the smallest detectable peak corresponds to approximately  $1 \cdot 10^{-4}$   $\mu$ l.

In Fig. 12 the sensitivity curves are shown, as plotted from the chromatograms obtained in this way. The values of the minimum detectable quantity for  $H_2$ ,  $O_2$  and  $N_2$  were calculated and found to be  $4.5 \cdot 10^{-12}$ ,  $1.4 \cdot 10^{-11}$  and  $1.6 \cdot 10^{-11}$  g/sec or in terms of concentration in the carrier gas  $9 \cdot 10^{-12}$ ,  $2.8 \cdot 10^{-11}$  and  $3.2 \cdot 10^{-11}$  g/ml respectively.

It should be noted, however, that the sensitivity curves based on the peak current are not at  $45^\circ$ , indicating that the detector is non-linear. This may possibly be attributed to the particular cell geometry, and could be improved by modifying the design of the electrode system.

## CONCLUSIONS

The results presented here show that the photoionization method, in which helium is used as both the discharge and the carrier gas, is suitable for the determination of minute quantities of inorganic gases. In the case of organic vapours,  $C_2$ - $C_4$  hydrocar-

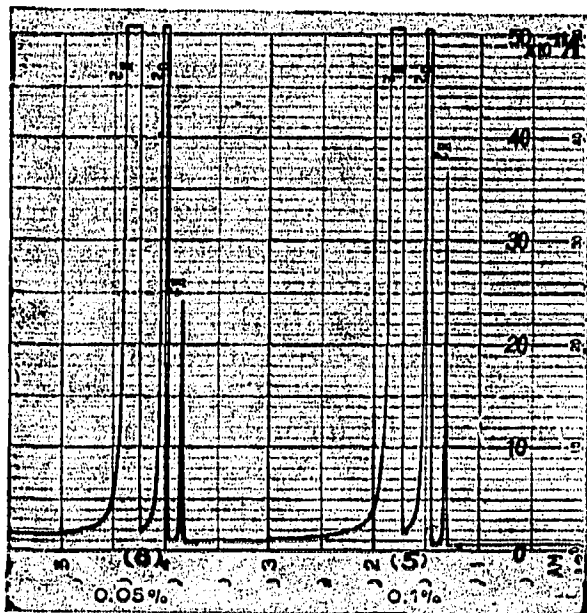


Fig. 11. Chromatograms of 0.1 ml of  $H_2$ -air mixtures. Full scale =  $50 \cdot 10^{-11}$  A. (5)  $H_2$  0.1%; (6)  $H_2$  0.05%. Carrier gas = He 30 ml/min; discharge gas = He 150 ml/min; discharge current =  $30 \mu A$ ; anode voltage = 100 V; column = molecular sieve 13X 1.5 m ( $20^\circ$ ).

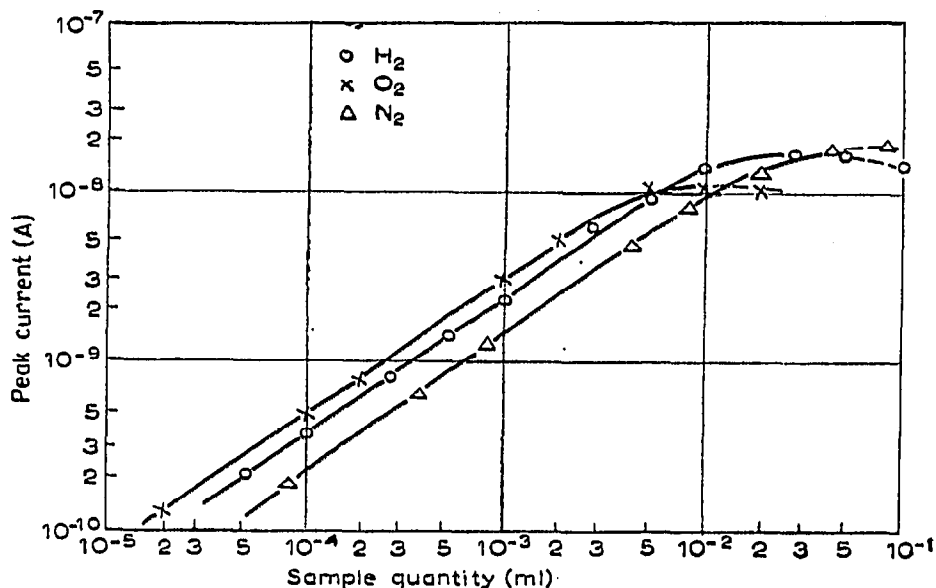


Fig. 12. Sensitivity curves for  $H_2$ ,  $O_2$  and  $N_2$ . Carrier gas = He 30 ml/min; discharge gas = He 150 ml/min; discharge current =  $30 \mu A$ ; anode voltage = 100 V; column = molecular sieve 13X 1.5 m ( $20^\circ$ ).

bon mixtures were tested and determined with satisfactory results, although this work is not reported in the present paper. These results depend on the fact that the helium discharge emits highly energetic ultraviolet radiation capable of ionizing molecules (with the exception of neon).

A most important point is the effect of impurities, which can absorb ultraviolet radiation. This gives rise to background current and, furthermore, reduces the ionization efficiency of the sample gas. An extreme degree of purification is therefore necessary to ensure satisfactory operation of the detector.

It is of interest to determine the concentration of the impurity encountered in our experiments. If we assume that the impurity was air, it is possible to estimate its concentration by injecting air of known quantity and relating the background current to the peak currents of the injected air. The concentration of the impurity in He in the sensing chamber is given by the formula:

$$C = \frac{I_B/u}{\{(I_{O_2} \times \sigma_{O_2}) + (I_{N_2} \times \sigma_{N_2})\}/W}$$

where  $C$  = concentration of the impurity.

$I_B$  = background current (A).

$u$  = sum of the flow rate of the carrier and the discharge gas (ml/sec).

$W$  = quantity of the injected air (ml).

$I_{O_2}, I_{N_2}$  = peak current of  $O_2$  and  $N_2$  of the injected air (A).

$\sigma_{O_2}, \sigma_{N_2}$  = band width of  $O_2$  and  $N_2$  peak (sec).

In order to obtain a numerical answer from this equation, we use the measured values obtained under the conditions of the sensitivity experiment (Fig. 12):  $I_B = 3 \cdot 10^{-10}$  A,  $u = 3$  ml/sec,  $W = 0.01$  ml,  $I_{O_2} = 5.3 \cdot 10^{-9}$  A,  $I_{N_2} = 8 \cdot 10^{-9}$  A,  $\sigma_{O_2} = 11$  sec and  $\sigma_{N_2} = 16$  sec. Substituting these values into the equation we get  $C = 5.3 \cdot 10^{-6}$ .

#### ACKNOWLEDGEMENTS

The author wishes to thank Dr. I. MAKINO, Director of the Naka works, Hitachi Ltd. and Mr. S. TAKEI for their interest and encouragement during the course of this investigation.

He wishes to express his indebtedness to Mr. S. D. NOREM of the Perkin-Elmer Corporation for his helpful discussions and his kind linguistic help in completing the original manuscript. He also wishes to thank Mr. M. YAMAMOTO for his useful discussions and Mr. I. ASAKAWA for his assistance in the measurements.

#### SUMMARY

This report describes studies of the photoionization detector which has been developed for the measurement of small amounts of components in the gas chromatographic analysis. By the use of helium as both discharge and carrier gas it is found that the detector can respond to permanent gases with high detection sensitivity, particularly when the helium is purified by the impurity traps.

Details are given of the operating characteristics, and the effects of impurity on the background current and the output signal is discussed.

## REFERENCES

- <sup>1</sup> M. YAMANE, *J. Chromatog.*, 9 (1962) 162.
- <sup>2</sup> M. YAMANE, *J. Chromatog.*, 11 (1963) 158.
- <sup>3</sup> J. E. LOVELOCK, *J. Chromatog.*, 1 (1958) 35.
- <sup>4</sup> J. E. LOVELOCK, *Nature*, 188 (1960) 401.
- <sup>5</sup> J. J. HOPFIELD, *Astrophys. J.*, 72 (1930) 133.
- <sup>6</sup> Y. TANAKA, A. S. JURSA AND F. J. LEBLANC, *J. Opt. Soc. Am.*, 48 (1958) 304.
- <sup>7</sup> R. E. HUFFMAN, Y. TANAKA AND J. C. LARRABEE, *J. Opt. Soc. Am.*, 52 (1962) 851.
- <sup>8</sup> R. E. HUFFMAN, Y. TANAKA, J. C. LARRABEE AND R. NOVACK, *Ionization Phenomena in Gases, II, Munich 1961*, North-Holland Publishing Co., Amsterdam, 1962, p. 1938.

*J. Chromatog.*, 14 (1964) 355-367